

Single-Molecule Interfacial Electron Transfer

Wilson Ho (Grant No. DE-FG02-06ER15826)

Department of Physics and Astronomy and Department of Chemistry

4129 Frederick Reines Hall

University of California, Irvine, CA 92697-4575

Telephone: (949) 824-3492; e-mail: wilsonho@uci.edu

Final Report

Program Scope

Interfacial electron transfer (ET) plays an important role in many chemical and biological processes. Specifically, interfacial ET in TiO_2 -based systems is important to solar energy technology, catalysis, and environmental remediation technology. However, the microscopic mechanism of interfacial ET is not well understood with regard to atomic surface structure, molecular structure, bonding, orientation, and motion. In this project, we used two complementary methodologies; single-molecule fluorescence spectroscopy, and scanning-tunneling microscopy and spectroscopy (STM and STS) to address this scientific need. The goal of this project was to integrate these techniques and measure the molecular dependence of ET between adsorbed molecules and TiO_2 semiconductor surfaces and the ET induced reactions such as the splitting of water. The scanning probe techniques, STM and STS, are capable of providing the highest spatial resolution but not easily time-resolved data. Single-molecule fluorescence spectroscopy is capable of good time resolution but requires further development to match the spatial resolution of the STM. The integrated approach involving Peter Lu at Bowling Green State University (BGSU) and Wilson Ho at the University of California, Irvine (UC Irvine) produced methods for time and spatially resolved chemical imaging of interfacial electron transfer dynamics and photocatalytic reactions. An integral aspect of the joint research was a significant exchange of graduate students to work at the two institutions. This project bridged complementary approaches to investigate a set of common problems by working with the same molecules on a variety of solid surfaces, but using appropriate techniques to probe under ambient (BGSU) and ultrahigh vacuum (UCI) conditions. The molecular level understanding of the fundamental interfacial electron transfer processes obtained in this joint project will be important for developing efficient light harvesting, solar energy conversion, and broadly applicable to problems in interface chemistry and surface physics.

Summary of Accomplishments

1. Single-Molecule Rotational and Vibrational Spectroscopy and Microscopy with the Scanning Tunneling Microscope This paper introduces a new method of single molecule imaging based on the rotational excitation of a hydrogen molecule trapped in the junction of a scanning tunneling microscope (STM) between the tip and the imaged molecule. Additionally imaging based on the vibrational excitation of the hydrogen molecule is also demonstrated. A single magnesium porphyrin molecule adsorbed on a

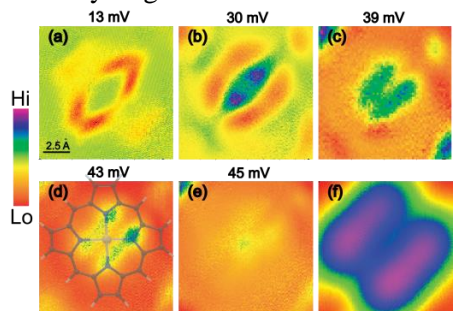


Figure 1. (a) – (e) IETS imaging of a MgP molecule on the $\text{Au}(110)2\times 1$ surface. In all images, the junction was set at $V_B = 50$ mV, $I_T = 1$ nA at each pixel, followed by disabling the feedback, ramping the bias to a chosen voltage, and recording d^2I/dV^2 signal by lock-in technique. A scaled model of MgP molecule is overlaid in (d) to show positions of the lobes in the image correspond to positions of the four nitrogen atoms. (f) For comparison, constant current topographic image.

Au(110) surface was imaged by inelastic electron tunneling spectroscopy with the STM of the trapped hydrogen molecule. We show that these rotational and vibrational images reveal the different chemical constituents inside the single magnesium porphyrin molecule. The technique is based on the sensitivity of the hydrogen rotational and vibrational energies and intensities to the positions of the magnesium porphyrin molecule as the tip scans over the molecule.

2. Rotational Spectromicroscopy: Imaging the Orbital Interaction between Molecular Hydrogen and an Adsorbed Molecule A new technique, rotational spectromicroscopy, is applied to visualize the interaction between a hydrogen molecule and single Mg-porphyrin molecule that can be reversibly charged and discharged on the surface of thin layers of Al_2O_3 grown on NiAl(110). When two molecules are close in space, intermolecular interaction can modify the potential energy surface and change the vibrational and rotational properties of each molecule. Molecular hydrogen can be trapped at low temperature within the tunneling junction of a scanning tunneling microscope (STM) by van der Waals force [Fig. 1(f)]. The $J=0 \rightarrow 2$ rotational excitation of the trapped hydrogen can be measured by spatially resolved inelastic electron tunneling spectroscopy (IETS) with the STM. The rotational excitation energy of hydrogen shifts from 45 meV to 42 meV energy when the tip is moved from Al_2O_3 substrate to over a neutral MgP molecule, indicating that the H-H bond is weakened by the intermolecular interaction. The spatial distribution of this shifted rotational excitation follows closely the lowest unoccupied molecular orbital (LUMO) of MgP, suggesting an interaction between the MgP LUMO and the hydrogen orbitals. In contrast, the interaction is not favored between the hydrogen and the singly unoccupied molecular orbital (SUMO) of the anionic MgP (MgP^-), because of the Coulomb repulsion arising from the extra electron in

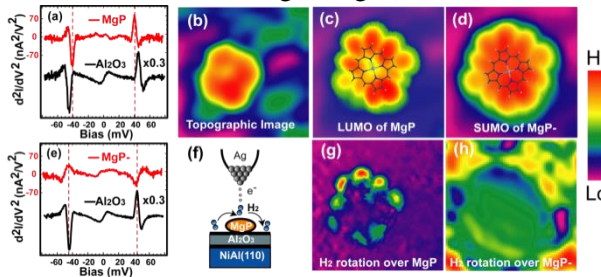


Figure 2. (a) IETS measurement of a trapped hydrogen molecule over neutral MgP (red) and Al_2O_3 substrate (black). (b) The topographic image of a MgP molecule that can be reversibly charged and discharged. (c) The topographic image of MgP taken at 500 mV bias which is at the onset of its LUMO. (d) The topographic image of MgP^- taken at 900 mV bias which is at the onset of its SUMO. (e) IETS measurement over MgP^- (red) compared to Al_2O_3 substrate (black). (f) Schematic diagram of a single molecule double-barrier junction with temporarily trapped H_2 . (g) d^2I/dV^2 image taken at 42 meV of trapped H_2 over neutral MgP. (h) d^2I/dV^2 image taken at 45 meV of trapped H_2 over MgP^- .

MgP^- that would limit the electron transfer critically important in the donor-acceptor interaction. The σ -donor nature of H_2 is further confirmed by its interaction with an electronegative Au atom adsorbed on the NiAl(110) surface. The possibility to trap a hydrogen molecule over an adsorbed molecule in the tunneling junction and to measure changes in the hydrogen rotational excitation spectrum leads to the realization of rotational spectromicroscopy as a new technique to image intermolecular interactions between hydrogen and another adsorbed molecule with atomic scale resolution, especially when the molecules are interacting in a non-planar geometries.

3. Trapping and Characterization of a Single Hydrogen Molecule in a Continuously Tunable Nanocavity The Scanning Tunneling Microscope (STM) tip and substrate forms a nano-cavity that can contain a single molecule. The geometry and size of the STM nano-cavity can be precisely tuned by changing the substrate topography and the tip-substrate distance, which modify the chemical environment of the

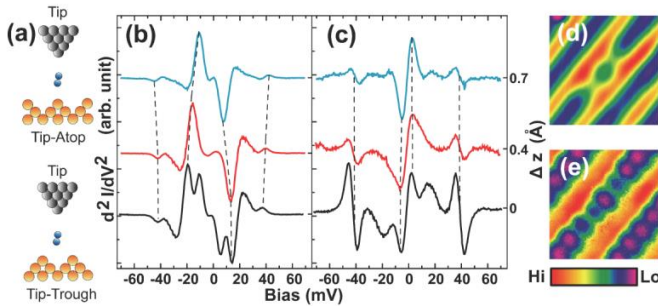
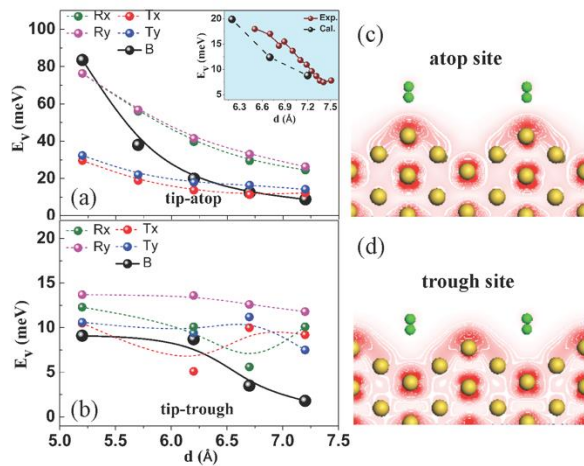


Figure 3. (a) Schematic diagrams of tip-atop cavity (top) and tip-trough cavity (bottom). (b-c) d^2I/dV^2 spectra of H_2 trapped in the tip-atop cavity (c) and tip-trough cavity (d) as the tip-substrate separation decreases by 0.7 Å. (d-e) Topographic images taken with (d) and without (e) a trapped hydrogen.

molecule in the cavity. Using inelastic electron tunneling spectroscopy (IETS) with STM and density functional theory (DFT) calculations, we investigated properties of a single H_2 molecule trapped in the STM nano-cavity form by the STM tip and the Au (110) surface. Au (110) has a 2×1 missing-row reconstruction and hence may form two different nano-cavities when the tip is parked above an Au atop row or over the trough between Au rows. Therefore, we may explore the effect of the nano-cavity's shape and size on chemical bonds. The topographic images taken after dosing molecular hydrogen reveal single atom resolution of the Au rows, while the resolution over the trough is almost unchanged. The STM-IETS measurements over the Au rows show strong vibrational excitation signal around 10 mV and relatively weaker rotational excitation signal at 42 mV. As the tip approaches the Au atop rows, the vibrational mode shifts to higher energy, whereas the rotational mode shifts to lower energy. Using the 3D rigid free rotor model, we found that the energy shift of the rotational mode from 43 to 41 meV corresponds to an expansion of the H-H bond length from 0.746 Å to 0.766 Å. The experimental data indicate that the H-Au interaction is enhanced and the H-H bond weakens as the dimension of the tip-atop nano-cavity decreases.



In contrast, the measurements for the tip positioned over the trough reveal very different features in the spectra. The IETS spectra show a vibrational mode of H_2 at 5 meV and a rotational mode at 42 meV. However, these two modes exhibit no resolvable shift when the tip-substrate distance shrinks.

DFT calculations are performed to provide an understanding of the distinct vibrational and rotational behavior of trapped H_2 in tip-atop and tip-trough cavities. All the vibrational energies increase monotonically for tip-atop cavity with the reduction of tip-substrate distance d , in good agreement with the experimental data. The increase of frequency for reduced d suggests an enhancement of the H-Au interaction at both ends of H_2 . In contrast, the bouncing mode in the tip-trough geometry is very soft and shows a weak dependence on the gap distance.

These distinct vibrational properties can be further understood from the electronic states at different sites on Au (110). DFT calculations indicate that the accumulation of the electronic states below H_2 molecule on atop site is larger than on the trough site, but their variations are smoother for the trough site. Thus, H_2

molecules adsorbed on atop sites are more sensitive to the rich electronic states below them than on trough sites when the STM tip approaches, leading to the rapid change of vibrational properties on atop site. Therefore, as the tip-substrate distance decreases, the H-H bond length will increase and tends to dissociate over atop rows, while not over trough rows. Combined STM-IETS measurements and DFT calculations allows establishment of microscopic understanding of the chemical process in tunable nano-cavities. Such precise control and the availability of clear insights provide the opportunity to explore chemical and biological processes with ultrahigh spatial resolution.

4. Nature of Asymmetry in the Vibrational Line Shape of Single-Molecule Inelastic Electron Tunneling Spectroscopy with the STM Single molecule vibrational spectroscopy with the scanning tunneling microscope (STM) was first realized experimentally in 1998 by inelastic electron tunneling spectroscopy (IETS). This new capability of the STM has served as a powerful tool for surface science research. The numerous experimental applications of STM and non-STM based IETS have mainly focused on the vibrational energy and intensity. Although asymmetry in the spectral line shape has been shown by theoretical calculations, it remained difficult to probe experimentally due to insufficient energy resolution limited by the high temperature of the sample and the microscope. In this work, we lowered the operation temperature to 600 mK and reported for the first time clear experimental observation of the asymmetry in the line shape of IETS. Furthermore, we demonstrated a way to control the line shape asymmetry through molecular manipulation by transferring a carbon monoxide molecule from the surface to the tip. It became possible to observe inversion symmetry for the spectral line shape when the coupling strengths of CO to the two sides of the asymmetric tunnel junction were reversed following the CO

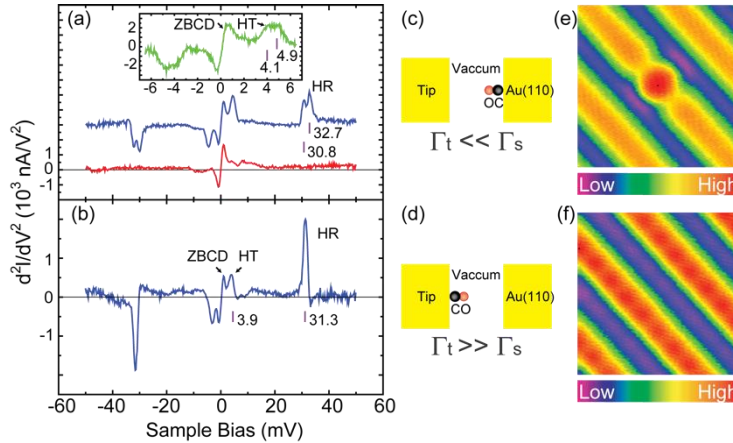


Figure 5. The asymmetric tunneling gap with CO adsorbed on two-fold symmetric Au(110) surface and to the tip. (a) Vibrational IETS spectrum taken with Au coated tip for single CO adsorbed on atop site. The upper curve (blue) is recorded over a CO molecule; the lower curve (red) is over Au(110) surface (spectrum is similar over the trough between two rows). Bias modulation: 1 mV at 471 Hz, and tunneling gap set point: $V = 20$ mV and $I = 1$ nA. The hindered rotational (HR) doublet are at 30.8 meV and 32.7 meV. Inset shows hindered translational (HT) doublet at 4.1 meV and 4.9 meV, taken with bias modulation 300 μ V at 471 Hz and tunneling gap set point: $V = 10$ mV and $I = 1$ nA. The zero bias conductance dip (ZBCD) at 1 meV is also observed over the Au surface. (b) STM-IETS with CO-terminated tip measured over the Au(110) surface. Bias modulation: 1 mV at 471 Hz, and tunneling gap set point: $V = 10$ mV and $I = 1$ nA. The HR-mode at 31.3 meV indicates that the tip is coated with Au atoms. Schematic diagrams for (c) metal tip probing single CO on Au(110) surface and (d) CO-terminated tip probing Au(110) surface. (e) Topography of CO adsorbed on Au(110) surface ($20 \text{ \AA} \times 20 \text{ \AA}$), taken with a metal tip. Set point: $V = 10$ mV and $I = 1$ nA. (f) Topography of CO-terminated tip probing the Au(110) surface ($20 \text{ \AA} \times 20 \text{ \AA}$). Set point: $V = 2$ mV and $I = 1$ nA.

transfer. These changes in the spectral line shape were reproduced with simulation of the theory behind STM-IETS. Rigorous validation of the current theoretical models is obtained with the availability of data on both the spectral intensity and line shape for the molecular vibrations. The present study puts on a firm foundation our understanding of the mechanisms of inelastic electron tunneling.

5. Quantitative Understanding of van der Waals Bonds by Analyzing the Adsorption Structure and Low-Frequency Vibrational Modes of Single Benzene Molecules on Silver The weak interactions between organic molecules and metal surfaces are essential for the control of many surface processes such as adsorption, catalytic reaction, sliding friction, epitaxial growth, and molecular electronics. Recent interest in weak bonds has inspired measurements of low-energy external vibrational modes of a molecule, either frustrated rotations (FR modes) or frustrated translations (FT modes) on the substrate. These modes typically have energies less than 15 meV, making it challenging to detect their spectroscopic features with conventional experimental techniques such as infrared reflection-absorption spectroscopy (IRAS), Raman spectroscopy, and high resolution electron energy loss spectroscopy (EELS) due to either insufficient energy resolution or low cross section. To this end, the low-temperature scanning tunneling microscope (STM) is an extremely powerful tool for the reliable characterization of the molecular adsorption configuration by the inelastic tunneling probe (itProbe) and the low-energy vibrational modes by inelastic electron tunneling spectroscopy (IETS). On the other hand, density functional theory (DFT) simulations with the inclusion of the van der Waals (vdW) correction can provide accurate results of the adsorption geometry and vibrational energies for quantitative comparison with experimental data. Synergistic STM-DFT exploration makes it possible to characterize and understand at a new level the nature of weak chemical bonds.

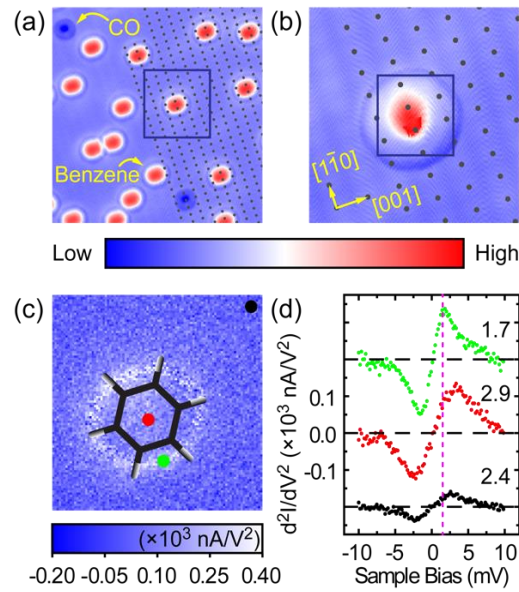


Figure 6. Imaging single benzene molecules. (a) and (b) Constant current topography of benzene (protrusions in red) and CO (depressions in blue) coadsorbed on Ag(110) at 600 mK, scanned with a CO-terminated tip: (a) set point: $V = 10$ mV and $I = 20$ pA, size: $80\text{\AA} \times 80\text{\AA}$, (b) zoom-in scan of the blue box in (a) and resolving surface Ag atoms, set point: $V = 1.5$ mV and $I = 100$ pA, size: $25\text{\AA} \times 25\text{\AA}$. (c) Constant height itProbe image of the boxed area in (b). Feedback was first turned off at the center of molecule with 10 mV sample bias and 80 pA tunneling current, then d^2I/dV^2 was recorded at 1.5 mV sample bias while the tip was held at a constant height throughout the imaging process, size: $9.0\text{\AA} \times 9.0\text{\AA}$. A scaled benzene structure is superimposed. (d) STM-IETS of CO on the Ag tip recorded at one of the three locations, indicated by the colored dots in (c). Bias voltage modulation was set to $1.5\text{ mV}_{\text{RMS}}$ at 311.11 Hz for recording d^2I/dV^2 signals with the lock-in amplifier.

In the present paper, we investigate the adsorption and vibrations of single benzene molecules on the Ag(110) substrate, using first-principles calculations along with sub-Kelvin STM measurements. The adsorption of benzene on various surfaces is a prototypical issue in chemistry and the nature of its interactions with the substrate tests the validity of different vdW's functionals. To date, the understanding of vibrational properties of aromatic molecules on metal surfaces is very limited. Our DFT calculations indicate that the interaction between benzene and Ag(110) is weak as suggested by the small adsorption energy: about -0.1 eV without vdW forces (about -0.8 eV with vdW forces.) Both STM image and theoretical calculation indicate that benzene prefers the short-bridge site of the Ag(110) surface and diffuses easily along the direction perpendicular to the closest packed Ag rows. With the high

spectroscopic resolution in the experiment and numerical reliability of the theory, we successfully identified the adsorption geometry and the low energy external vibrational modes of benzene on the Ag substrate. Furthermore, we could associate the vibrational energies of these frustrated translational and frustrated rotational modes with the strength of the adsorbate-substrate interaction, i.e. the binding energy of the molecule on the surface. The precise measurements coupled with rigorous calculations enabled definitive understanding of weakly interacting systems.

6. Tunneling Electron Induced Charging and Light Emission of Single Panhematin Molecules This paper probes the electronic and optical properties of single molecules of panhematin or hemin. The use of tunneling electrons in a low temperature scanning tunneling microscope in ultrahigh vacuum enables sub-Ångström spatial resolution in the initial injection of an electron into the excited state of a molecule. It is found that an electron can be transferred to the molecule to convert it to an anion. Optical transition occurs following the tunneling of another electron into the anion, thus making the initial state to be a transient doubly charged state. Another unusual occurrence is that the final state is the continuum states near the Fermi level of substrate. Thus the novelty of this paper lies in the coupling of a discrete doubly charged state to a continuum in a radiative decay of a single molecule probed with sub-Ångström spatial resolution.

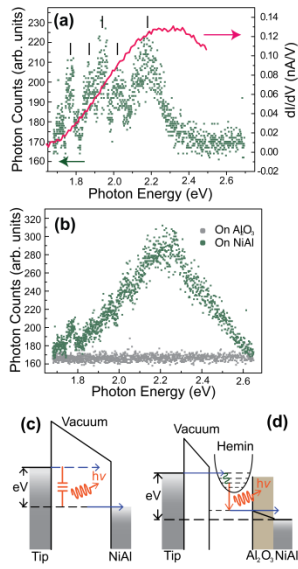
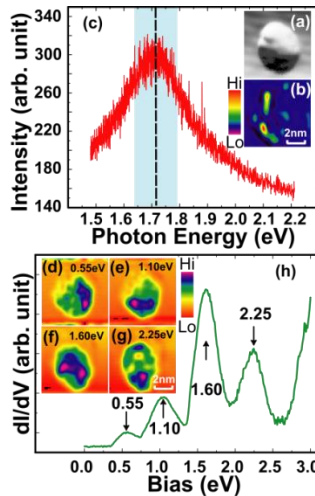


Figure 7. Light emission from hemin molecules. (a) Photon emission spectrum (green curve) collected over center of hemin molecule. Tunnel junction was set at $V_B = 2.5$ V, $I_T = 1$ nA, with the CCD exposed for 10 mins. The dI/dV spectrum (magenta curve) of same molecule over same energy range is overlaid on top. Emission peaks from vibronic transitions are shown based on multi-peak Lorentzian fit. The energy positions are 1.77 eV, 1.87 eV, 1.94 eV, 2.02 eV, and 2.18 eV. (b) Light emission spectra from the NiAl (110) substrate (green curve) and Al₂O₃ layer (grey curve). Both spectra were taken with same set point as in (a). CCD was exposed for 100 s for NiAl (110) and 10 mins for Al₂O₃. (c) – (d) Schematic diagrams of light emission mechanisms on substrate (c) and over hemin molecule (d). Over metal substrate, light emission occurs through inelastic electron tunneling (IET) process, exciting a plasmon in the junction. Over hemin, emission mechanism involves intramolecular radiative transitions between molecular vibronic states.

7. Tunneling Electron Induced Light Emission from Single Gold Nanoclusters Metallic nano-clusters with dimensions of ~ 10 nm are found in numerous catalysts. These dimensions are at least an order of magnitude smaller than the wavelengths of visible and UV light used typically in photocatalysis. In the near-field, light can couple effectively to plasmon modes of the nano-clusters, facilitating photochemistry to occur. In order to utilize this coupling, it is necessary to understand the energy and spatial distribution of these plasmon modes associated with the nano-clusters. In this project, we have used the unique spatial resolution of the STM to characterize the electronic and optical properties of Au nano-clusters grown on Al₂O₃ surface. When dosed at room temperature, Au atoms diffuse and form nano-clusters on the oxide surface. The nano-clusters ranged 3~7 nm in size and have fairly uniform shape. Electronic properties of the nano-clusters are studied using scanning tunneling spectroscopy (STS). The dI/dV spectrum of an Au nano-cluster, reveals features similar to those for a one-dimensional atomic chain exhibiting “particle-in-a-box” properties. The dI/dV images at different electronic states reveal highly localized structures as expected from quantum confinement effects. Light emission from single and dimeric nano-clusters are collected by a lens inside the vacuum chamber and guided to a nitrogen cooled charged-coupled device (CCD) equipped with a spectrograph. Topography and light emission from a single 4 nm nano-cluster were recorded. The light emission spectrum and imaging show a highly localized plasmon mode at 1.71



eV. Other nano-clusters of varying sizes from 3 nm to 7 nm show shift and splitting of the main plasmon peak.

Figure 8. (a)–(c) Topography and light emission of a single Au nano-cluster. Light emission spectrum shows single plasmon peak at 1.71 eV. The light emission image in (b) is taken with photon energy ranging from 1.64 eV to 1.79 eV (shaded blue region). (d)–(h) dI/dV spectrum for same nano-cluster, and dI/dV imaging at voltages corresponding to peaks in the spectrum.

We also investigated light emission from nano-cluster dimers (two clusters situated close to each other). Interestingly, no obvious enhancement effect to the light emission is observed in between the clusters. They behave as if they are isolated and do not interact with each other. These results suggest

that the emitted light is polarized, and the polarization is predominantly parallel to the surface in the dimer gap. This polarization direction does not interact with the plasmon mode of the tip, which is perpendicular to the surface.

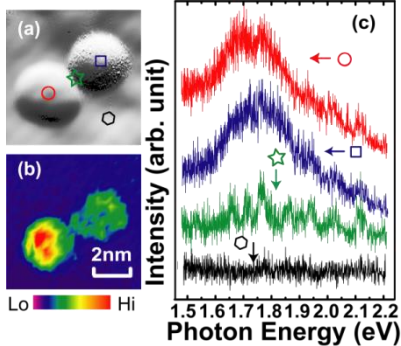


Figure 9. (a) Topographic image of a dimer of Au nano-clusters. (b) Light emission image integrated in wavelength for the Au nano-clusters dimer. The tunnel junction is set at 3V, 3nA. Exposure time at each pixel is 3s. (c) Light emission spectra taken above each Au nano-cluster, between the dimer, and over Al_2O_3 . The positions are marked in panel a. The tunnel junction is set at 3V, 3nA. Exposure time is 1000s.

8. Imaging van der Waals Interactions This paper provides new understanding into the nature of the van der Waals (vdW) bond through first time imaging of the bond and analyses by density functional calculations. Self-assembly of Xe atoms on a metal surface presents an ideal vdW system for fundamental studies. The fact that they form a close packed hexagonal structure suggests the presence of interatomic attraction, i.e. bonding, that is responsible for the self-assembly. The scanning tunneling microscope (STM) exclusively probes the Xe structure at the surface and is practically blind to the underlying substrate. The vdW bond is imaged by a unique application of the STM as an inelastic tunneling probe (itProbe) that is based on detecting changes in the lowest energy vibration of a CO molecule attached to the tip as it senses the spatial variations of the potential over the Xe layer. The spatial variations in the potential track the bonds between atoms.

Traditionally, vdW bond has been associated with charge fluctuations that lead to interactions of the instantaneous dipole with its induced counterpart in an adjacent entity. On the other hand, when atoms are in the vicinity of each other, electron redistribution is bound to occur, which can be captured by STM measurements and DF calculations. The present paper reports real-space imaging of vdW bonds between adjacent Xe atoms, and the DF calculations (with vdW correction) reveal the shift of electron density toward the region between adjacent Xe atoms. Directionality is observed in the itProbe images and can be correlated with the ridges of the potential energy surface associated with the charge density. Comparison of experiment and theory conclude that ridges of charge density in the two-dimensional plane above the Xe layer define the vdW bonds. These results add new insights for the formation of extremely weak

chemical bonds and provide a universal understanding into the nature of the chemical bonds as charge rearrangement between atoms and the associated potential perturbation in space. Unlike covalent bond formed by carbon, the angle between two adjacent vdW bonds is not constrained and can take on continuous values depending on the positions of the adjacent atoms. A vdW bond in simple systems as Xe is formed by connecting the centers of the two interacting atoms.

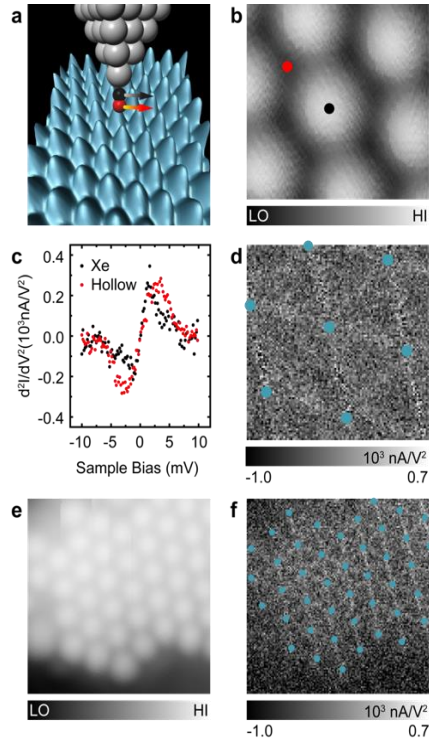


Figure 10. Imaging connectivity of vdW interactions with itProbe. a. Schematic of itProbe showing the CO-tip over a self-assembled Xe monolayer while monitoring the hindered translational vibration of CO (C: black ball, O: red ball). The intensity at a chosen fixed bias is monitored at each pixel in composing an itProbe image. b. A topographic image obtained by a CO-tip with the tunneling gap set at 0.1 nA and 0.1 V, showing the hexagonal close pack arrangement of Xe atoms. c. STM-IETS of CO-tip at set point 0.1 nA and 10 mV, showing the hindered translational mode, recorded at the two positions indicated in b. d. Constant current itProbe image of Xe atoms in b with bias set at 1.6 mV. At each pixel, the tunneling gap is chosen with set point 0.1 nA and 10 mV. Feedback is then turned off, followed by decreasing the bias to 1.6 mV for recording the d^2I/dV^2 vibrational signal. e. Topographic image for part of a self-assembled island with set point 0.1 nA and 0.1 V. f. Corresponding constant height itProbe image of the same area as e. The constant tunneling height is chosen with set point of 0.1 nA and 0.1 V over the central Xe atom, followed by turning off the feedback. Signal acquisition is initiated after decreasing the bias to 1.5 mV and bringing the tip 1.6 Å closer to the surface. For ease of visualization, the positions of the Xe atoms are indicated by the blue dots.

9. Imaging the Halogen Bond in Self-Assembled Halogenbenzenes on Silver Interactions between molecules have noncovalent character, in contrast to the chemical bonds between atoms within a molecule. Noncovalent interactions include the hydrogen bond, van der Waals' forces, and the halogen bond. Of these three noncovalent interactions, the halogen bond has received the least attention despite its wide ranging importance in biological systems, drug discovery, and polymer conformations. More specifically, halogen bond directs ligand recognition by proteins and conformations in DNA. Despite its prevalence, the formation of the halogen bond remains surprising. This unexpected attractive interaction strikes home for fully halogenated molecules. The highly electronegative halogens X in the polarized A-X bonds are negatively charged and electrostatic repulsion would make halogen bond unfavorable. In this study, we studied hexafluorobenzene (C_6F_6) and hexabromobenzene (C_6Br_6), and contrasted with benzene (C_6H_6). The hexahalogenbenzene self-assemble into ordered islands, in contrast to the individually adsorbed benzene. We applied the unique technique of the inelastic tunneling probe (itProbe) based on a 600 mK STM and in combination with DFT calculations to reveal the nature of the halogen bond that is responsible for the self-assembly. This study further suggests that in extended molecular systems, intermolecular interactions are more complex but could be understood from the potential energy surface as probed by monitoring minute changes in the vibration of a CO molecule on the STM tip. The halogen bond suggests that the formation of chemical bonds can be generally described as perturbation in space of the potential surface associated with the rearrangement of the electron density. The novelty and the broad implication of this study lies in the elucidation of the halogen bond and the conceptual framework in understanding the nature of the chemical bond.

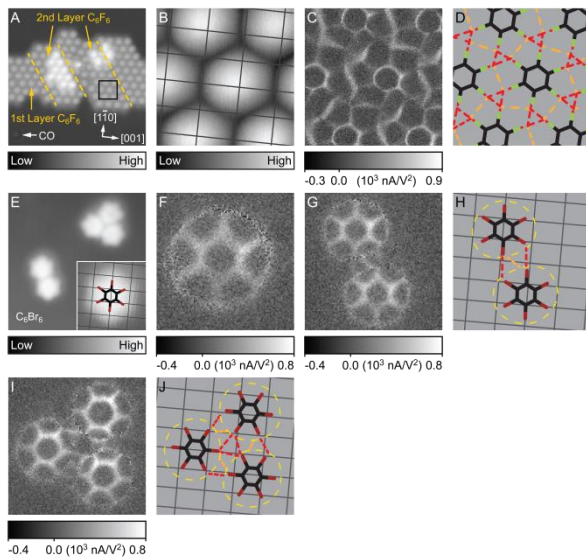


Figure 11. Self-assembled C_6F_6 island and C_6Br_6 clusters on a $Ag(110)$ surface. (A) Constant current topography of C_6F_6 island and co-adsorbed CO molecule on $Ag(110)$ scanned with a CO-terminated tip. Domain boundaries are indicated by yellow dashed lines. (B) Constant current zoomed in topography of the black square area in A, the gray rectangular grid represents the underlying $Ag(110)$ lattice with surface atoms at the line intersections. (C) Constant current itProbe imaging at 1.2 mV of the same area as in B. (D) Schematic diagram of the itProbe image in C. Intermolecular bonding network highlighted by red and orange dashed lines. (E) Constant current topography of C_6Br_6 trimer, dimer and monomer (inset) scanned with a CO-tip. (F), (G) and (I) Constant height itProbe images at 1.5 mV of the monomer, dimer and trimer shown in E. (H) and (J) Schematic diagram of the C_6Br_6 dimer and trimer shown in E. The rectangular grids in E, H and J show the $Ag(110)$ lattice.

Publications Acknowledging DOE Support

1. A. Yu, S.W. Li, G. Czap, and W. Ho, "Single-Molecule Rotational and Vibrational Spectroscopy and Microscopy with the Scanning Tunneling Microscope," *J. Phys. Chem. C* **119**, 14737-14741 (2015).
2. S.W. Li, A. Yu, G. Czap, D.W. Yuan, R. Wu, and W. Ho, "Rotational Spectromicroscopy: Imaging the Orbital Interactions Between Molecular Hydrogen and an Adsorbed Molecule," *Phys. Rev. Lett.* **114**, 206101 (2015).
3. H. Wang, S.W. Li, H.Y. He, A. Yu, F. Toledo, Z. Han, W. Ho, and R. Wu, "Trapping and Characterization of a Single Hydrogen Molecule in a Continuously Tunable Nanocavity," *J. Phys. Chem. Lett.* **6**, 3453-3457 (2015).
4. C. Xu, C.L. Chiang, Z. Han, and W. Ho, "Nature of Asymmetry in the Vibrational Line Shape of Single-Molecule Inelastic Electron Tunneling Spectroscopy with the STM," *Phys. Rev. Lett.* **116**, 166101-1-4 (2016).
5. D. Yuan, Z. Han, G. Czap, C. Chiang, C. Xu, W. Ho, and R. Wu, "Quantitative Understanding of van der Waals Interactions by Analyzing the Adsorption Structure and Low-Frequency Vibrational Modes of Single Benzene Molecules on Silver," *J. Phys. Chem. Lett.* **7**, 2228-2233 (2016).
6. A. Yu, S.W. Li, B. Dhital, H.P. Lu, and W. Ho, "Tunneling Electron Induced Charging and Light Emission of Single Panhematin Molecules," *J. Phys. Chem. C* **120**, 21099-21103 (2016).
7. A. Yu, S.W. Li, G. Czap, and W. Ho, "Tunneling-Electron-Induced Light Emission from Single Gold Nanoclusters," *Nano Lett.* **16**, 5433-5436 (2016).
8. Z. Han, X. Wei, C. Xu, C.-L. Chiang, Y. Zhang, R. Wu, and W. Ho, "Imaging van der Waals Interactions," *J. Phys. Chem. Lett.* **7**, 5205-5211 (2016).
9. Z. Han, G. Czap, C.-L. Chiang, C. Xu, P.J. Wagner, X. Wei, Y. Zhang, R. Wu, and W. Ho, "Imaging the Halogen Bond in Self-Assembled Halogenbenzenes on Silver", *Science* **358**, 206-210 (2017).